Bulletin of the Seismological Society of America, Vol. 107, No. 3, pp. 1451–1463, June 2017, doi: 10.1785/0120150330

Ⓔ

Performance Evaluation of the Earthquake Detection and Classification Algorithm $2(t_S–t_P)$ of the Seismic Alert System of Mexico (SASMEX)

by Armando Cuéllar,* Gerardo Suárez, and J. M. Espinosa-Aranda

Abstract A performance evaluation of the detection and classification algorithm for earthquake early warning $2(t_S–t_P)$ was conducted to test its reliability and robustness. The Seismic Alert System of Mexico (SASMEX) has used this algorithm since 1991. The algorithm estimates the rate of seismic energy released during two times the $(t_S–t_P)$ period. Based on the energy released, it estimates an empirical magnitude range related to m_b. Depending on the estimated m_b, either preventive or public alerts are issued. In this article, *post facto* tests are presented for 61 earthquakes for which SASMEX issued an alert. The algorithm was also tested on 31 earthquakes ($M_w > 6.0$) that occurred in the Mexican subduction zone from 1985 to 2014. These earthquakes occurred outside the coverage of the SASMEX instruments at the time. This dataset includes the 19 September 1985 M_w 8.1 Michoacán earthquake and the 9 October 1995 M_w 8.0 Colima event. The algorithm was tested also on two great earthquakes: the 22 February 2010 M_w 8.8 Maule, Chile, earthquake and the 11 March 2011 M_w 9.0 Tohoku, Japan, event. The results of the evaluation of 144 acceleration records of the 61 earthquakes detected from the SASMEX network indicate that 92% of the accelerograms of earthquakes with $m_b > 6.0$ have errors in the prediction of magnitude of less than ±0.5, and 83% for $m_b > 5.5$. Also, the tests conducted on the 59 acceleration records of 31 earthquakes with $M_w \geq 6.0$ indicate that in all cases, with the exception of one strong-motion record, the events are classified as $M_w \geq 6.0$. Thus, the algorithm shows a high level of reliability and robustness. Although the algorithm underestimates the magnitudes of large earthquakes, these events are identified and classified as $M_w \geq 6.0$. Thus, an alert would be issued for these great earthquakes.

Electronic Supplement: Table of earthquake parameters, performance of Seismic Alert System of Mexico (SASMEX), and specific performance evaluation of the $2(t_S–t_P)$ algorithm.

Introduction

Considering the damage suffered by Mexico City after the 19 September 1985 earthquake (e.g., Rosenblueth, 1986; Esteva, 1988), the scientific community proposed in 1986 the creation of a Seismic Alert System for Mexico City (SASMEX; CONACYT-NRC, 1986). The goal was to alert the city of earthquakes originating in the subduction zone along the Pacific coast of Mexico. The possibility of a future great earthquake in the Mexican subduction zone raised local and federal authorities awareness of the need to develop an early warning system. As a result, the Centro de Instrumentación y Registro Sísmico, A.C. (CIRES, Center for Instrumentation and Seismic Recording) initiated the development of the SASMEX in 1989. The objective is to warn the population of the capital city of Mexico about the occurrence of important earthquakes detected by a network of free-field acceleration stations distributed along the coast (Fig. 1).

Mexico City is an ideal location to implement a seismic alert system. The soft clays on which the city is built cause large ground-motion amplifications, as was the case during the 1985 earthquake. This amplification can lead to strong ground motion, even for distant earthquakes for which warning times can be long. SASMEX was conceived to identify future large-magnitude earthquakes along the subduction zone and automatically alert the population of Mexico City prior to the arrival of the incoming seismic waves. The

*Also at Centro de Instrumentación y Registro Sísmico, Anaxágoras 814 Colonia Narvarte, México CDMX 03020.

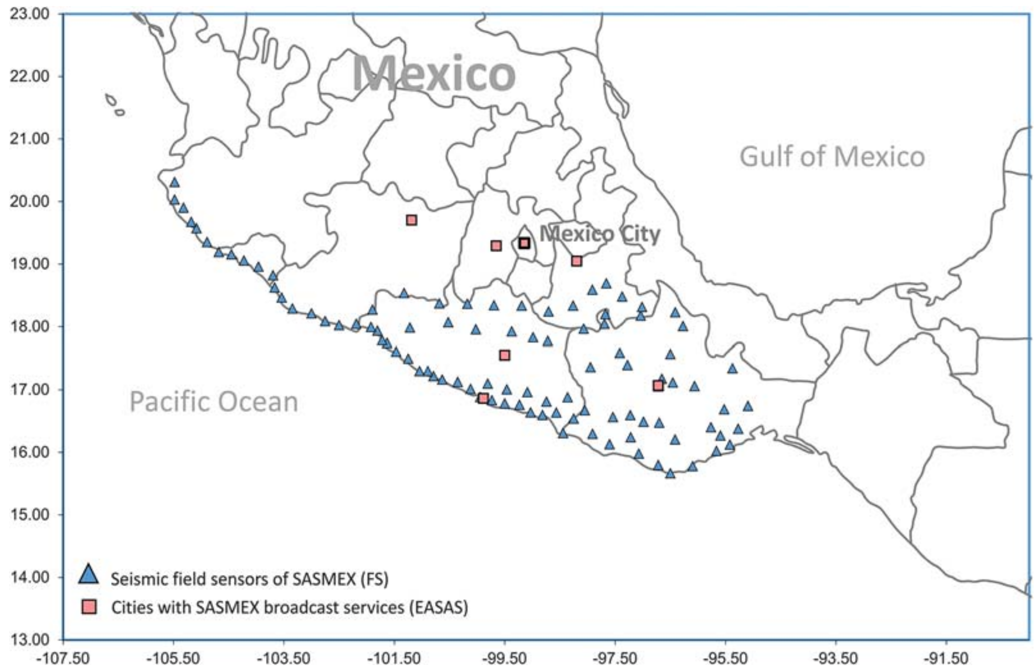

Figure 1. Current distribution of Seismic Alert System of Mexico (SASMEX) strong-motion stations (triangles) and alternate emitters of seismic warnings designed to disseminate the alert in various Mexican cities (squares).

system takes advantage of the slower travel time of seismic waves relative to the rapid transmission of data via radio.

In Mexico City, the warning time allowing the population and authorities to react to the possibility of strong shaking due to earthquakes in the subduction zone, may be as large as 60–90 s. The most recent earthquake with magnitude $M_w > 7.0$ in the subduction zone, immediately to the south of Mexico City, took place in 1911. Therefore, it is generally assumed that an important accumulation of stress probably exists in this segment of the coast of Guerrero, called the Guerrero gap (McCann *et al.*, 1979; Singh *et al.*, 1981). This was the reason why the location of the original seismic coverage of the system was on the Guerrero gap.

This article presents a systematic evaluation of the primary detection and classification algorithm used by SASMEX, called the $2(t_S–t_P)$ algorithm. This algorithm calculates the rate of energy released during twice the elapsed time between the arrival of the *P* and *S* waves. Based on the growth rate of the seismic energy, the algorithm classifies events into three magnitude bins ($m_b < 5.5$, $5.5 \leq m_b < 6.0$, and $m_b \geq 6.0$) and makes the decision whether to issue an alert. The algorithm was developed originally using a training set of earthquakes recorded by the strong-motion records of the Guerrero network (Anderson and Quaas, 1988). Although it has been modified slightly over time, the $2(t_S–t_P)$ algorithm remains the basis on which seismic alerts have been issued by SASMEX since 1991.

In this study, we evaluate the $2(t_S–t_P)$ algorithm as it is used today and test it retroactively on the strong-motion database of accelerograms recorded by SASMEX since its inception in 1991. Also, we evaluated its performance for all earthquakes with $M_w \geq 6.0$ that have occurred along the Mexican subduction zone since 1985. These earthquakes lie outside the original coverage of SASMEX. To this end, we use accelerograms recorded by various agencies. Among these events is the 19 September 1985 earthquake, which caused great damage in Mexico City and prompted the effort to develop an early warning system.

In addition, a study was made of the performance of the $2(t_S–t_P)$ algorithm on two great earthquakes: the 2011 M_w 9.0 Tohoku, Japan, and the 2010 M_w 8.8 Maule, Chile, earthquakes. This was done to evaluate the earthquake classification criteria of the $2(t_S–t_P)$ algorithm in the case of a future great magnitude earthquake. Although the epicentral distances of the Tohoku and Maule earthquakes to the closest strong-motion stations are very large and outside of the design parameters of the $2(t_S–t_P)$ algorithm, we use these two earthquakes as extreme tests to verify the robustness and performance of the algorithm in the case of great magnitude earthquakes. The same evaluation criteria are used for the three datasets.

It is important to emphasize that the $2(t_S–t_P)$ algorithm presented here does not estimate a hypocentral location or the source characteristics of the earthquake. It detects the earthquakes in real time and classifies them into three magnitude bins. For this, it requires only two nearby stations confirming the seismic energy growth to issue an alert. Many of the existing seismic early warning systems attempt a more detailed characterization of ongoing earthquakes and require longer times and a larger number of stations to issue a warning. The algorithm Earthquake Alarm Systems (ElarmS), for example, uses at least four stations to confirm an alert (Allen *et al.*, 2009).

The most important conclusion derived from this analysis is that the $2(t_S–t_P)$ algorithm used by SASMEX would have been able to identify all earthquakes with magnitudes $M_w \geq 6.0$ in the subduction zone of Mexico based only on two strong-motion records near of the epicenter; with only one exception, it would have relayed a warning signal to the population of Mexico City. Similarly, in the case of extreme earthquakes, such as the Chile and Tohoku events ($M_w > 8.5$), the algorithm would have issued a seismic alert, even though the available strong-motion records for these earthquakes are far from the epicenter.

Description of SASMEX

During 2011 and 2012, SASMEX expanded its limited coverage, from the 12 original stations commissioned in 1991 along the southern coast of the state of Guerrero to a network of 97 stations distributed along the Mexican Pacific coast, from the state of Jalisco to the state of Oaxaca (Fig. 1). Also, stations were distributed along 18° N to monitor the seismic activity within the subducted Cocos plate (Fig. 1; Cuéllar *et al.*, 2014). In 2012, SASMEX integrated the Seismic Alert System of the state of Oaxaca that started operating in 2003 (Espinosa-Aranda *et al.*, 2009). Both systems currently constitute the SASMEX (Cuéllar *et al.*, 2014).

In 1991, CIRES was instructed by the authorities to broadcast a preventive alert to owners of dedicated receivers of the system in case of an earthquake with body-wave magnitude $5.0 < m_b < 6.0$. In the case of earthquakes with $m_b \geq 6.0$, SASMEX was instructed to relay a public alert that, in addition to being received by the dedicated receivers, would be broadcast via the radio and television stations that volunteered to disseminate the seismic alert to the public since 1993 (Espinosa-Aranda *et al.*, 1995). Since 2015, the government of Mexico City broadcasts the public alerts through a network of thousands of loudspeakers distributed throughout the city. Today, the alerting policy for the $2(t_S–t_P)$ algorithm is as follows: no alert for earthquakes with $m_b < 5.5$; relay a preventive alert if $5.5 \leq m_b < 6.0$; and issue a public alert when $m_b \geq 6.0$.

The seismic field sensor (FS) stations consist of three-component accelerographs. The broadcast of an alert requires the confirmation of at least two nearby FS stations. In addition to classifying the earthquakes based on the seismic energy released into magnitude ranges or bins, the process of broadcasting the alert takes into account the distance that exists between the first two FS stations detecting the earthquake and the city to be alerted. Today, in addition to Mexico City, the cities of Acapulco, Chilpancingo, Oaxaca, Morelia, Puebla, and Toluca broadcast seismic alerts (Fig. 1).

The Algorithm $2(t_S–t_P)$

Background

The detection and classification algorithm for large earthquakes with which SASMEX has operated since 1991 is known as the $2(t_S–t_P)$ algorithm. It is structured into four modules:

1. *P*- and *S*-phase arrival identification, which in turn determines the $2(t_S–t_P)$ time;
2. estimation of parameters reflecting the seismic energy released in the period $2(t_S–t_P)$;
3. classification of the event into magnitude ranges based on the estimated seismic energy released; and
4. decision-making processes whether or not to issue an alert, be it preventive or public.

P- and *S*-Phase Arrival Identification

The FS stations identify the arrival of the *P* and *S* waves based on two independent approaches: average square input (ASI) and vertical to horizontal (V/H). ASI is based on the sum of quadratic averages of the amplitude of the acceleration records (Espinosa-Aranda, *et al.*, 1995). V/H was used by the Japanese railway earthquake alert system, Urgent Earthquake Detection and Alarm System (Nakamura, 1996). Both methods are described below.

The ASI Method

The original ASI employed by SASMEX (Espinosa-Aranda *et al.*, 1992) processed the sum of the quadratic amplitude of the three strong-motion components of an accelerometer (longitudinal X_l, transverse X_t, and vertical X_v) at a sampling rate of 50 Hz and with a resolution of 10 bits in an average time window of 32 samples. Subsequently, because of increase of the resolution in the FS stations to 12 bits and of the sampling rate to 100 Hz, the average time window was reduced to 16 samples and separately calculates the quadratic amplitude on the horizontal and vertical components (equations 1 and 2). Thus, the average seismic energy growth, expressed as the squared sum of the amplitude of the seismic waves, is estimated as a function of time:

$$\mathrm{ASIH}_{16}(i) = \frac{1}{16}\sum_{i-15}^{i}[X_l^2(i) + X_t^2(i)] \tag{1}$$

$$\mathrm{ASIV}_{16}(i) = \frac{1}{16}\sum_{i-15}^{i}X_v^2(i), \tag{2}$$

in which i is the current sample and X_l, X_t, and X_v are the acceleration amplitudes of the three orthogonal channels: longitudinal, transverse, and vertical.

The V/H Method

The V/H method, defined by equations (3) and (4) (Nakamura, 1996) is used in parallel to confirm the arrival of the *P* and *S* waves:

$$\mathrm{V}(i) = \mathrm{V}(i-1) + X_v^2(i) \tag{3}$$

$$\mathrm{H}(i) = \mathrm{H}(i-1) + X_l^2(i) + X_t^2(i). \tag{4}$$

When the ratio V/H > 1, the P wave is predominant, whereas in the case of V/H < 1, the predominant presence of the S wave is inferred (Nakamura, 1996). Identification of the P- and S-phase arrivals is not always stable because of the characteristics of each particular earthquake and the effect of local seismic noise at the site. Therefore, we follow Nakamura (1996) in weighting the vertical and horizontal amplitudes with coefficients α_1, α_2, α_3, β_1, β_2, and β_3. These weighting coefficients range in value from 0 to 1 and are determined empirically for each sensing station based on recorded accelerograms (Nakamura, 1996). The V/H quotients are then estimated as follows:

$$\frac{\alpha_1 \mathrm{V}}{\beta_1 \mathrm{H}} \text{ is calculated from } t_P + 0.5 \text{ s;}$$

$$\frac{\alpha_2 \mathrm{V}}{\beta_2 \mathrm{H}} \text{ is calculated from } t_P + 0.5 \text{ to } t_P + 1.0 \text{ s;}$$

and

$$\frac{\alpha_3 \mathrm{V}}{\beta_3 \mathrm{H}} \text{ is calculated from } t_P + 1.0 \text{ to } t_P + 24.0 \text{ s.}$$

Then, the arrival of the P and S waves is defined when all of the following criteria are met:

$$\begin{cases} P: \mathrm{ASIV}_{16} > u_{P1}; V > u_{P2}; \frac{\alpha_1 \mathrm{V}}{\beta_1 \mathrm{H}} > 1; \frac{\alpha_2 \mathrm{V}}{\beta_2 \mathrm{H}} > u_{P3}; T_P > 1 \text{ s} \\ S: \mathrm{ASIV}_{16} > u_{S1}; \frac{\alpha_3 \mathrm{V}}{\beta_3 \mathrm{H}} > u_{S2}; T_S < 24 \text{ s} \end{cases}, \quad (5)$$

in which u_{Pi} and u_{Sk} are the thresholds of the seismic signals estimated dynamically in the following manner:

$$u_{P1} = \frac{1}{100} \sum_{t_P-99}^{t_P} X_v^2(i);$$

$$u_{P2} = \max[\mathrm{V}(i)]_{i=t_P-16}^{t_P};$$

$$u_{P3} = \frac{1}{25} \sum_{i=t_P+50}^{t_P+75} \frac{\mathrm{V}(i)}{\mathrm{H}(i)};$$

$$u_{S1} = 2 \max[\mathrm{ASIH}_{16}(i)]_{i=t_P}^{t_P+200};$$

$$u_{S2} = \min\left[\frac{\mathrm{V}(i)}{\mathrm{H}(i)}\right]_{i=t_P+50}^{t_P+150}.$$

The detection process of the P wave starts in the instant t_p, and the identification is based on the following criteria: (1) when ASIV_{16} exceeds the average threshold u_{P1}, dynamically calculated every minute, and reflecting the noise level at the site; (2) when the value of V exceeds the threshold u_{P2} and the parameter $\frac{\alpha_1 \mathrm{V}}{\beta_1 \mathrm{H}}$, proportional to the growth rate of the signal, is larger than 1; and (3) $\frac{\alpha_2 \mathrm{V}}{\beta_2 \mathrm{H}}$ exceeds a threshold u_{P3}. These conditions are expected to occur within an observation window T_p of maximum duration of 1 s.

The detection of the S wave is declared when the following conditions are met: (1) ASIV_{16} should exceed the threshold u_{S1}, calculated dynamically, in terms of the maximum peak values generated by the P waves. The value u_{S1} is updated every time a new maximum peak value of ASIH_{16} is observed; (2) when $\frac{\alpha_3 \mathrm{V}}{\beta_3 \mathrm{H}} < u_{S2}$. The value of u_{S2} is calculated dynamically based on the minimum V/H after the P-wave detection. The algorithm has a maximum observation time of $T_S < 24$ s after the detection of the P wave to identify the S wave.

Functions ASIV_{16} and ASIH_{16} are shown graphically in Figure 2 and demonstrate the S wave identified at the Cacalutla station during the 13 April 2007 M_w 6.0 Atoyac, Guerrero, earthquake (Fig. 2). The epicentral distance of this station is ~40 km from the epicenter.

Evaluation of the P and S Automatic Arrival-Time Determinations

The sensing stations of SASMEX have no absolute time signals, because they are designed specifically for the purpose of a seismic alert. Furthermore, the other agencies running strong-motion stations in Mexico do not pick P and S phases on the accelerograms on a routine basis. Thus, to demonstrate the performance of the phase-picking algorithms described above, we present the strong-motion records of selected events and the times in which the arrival of the P and S phases were automatically selected (Fig. 3).

A more complete set of strong-motion records and the time of the automatic P- and S-phase picks on several accelerograms used in this analysis are shown also in Ⓔ Figures S1 and S2, available in the electronic supplement to this article. These figures demonstrate that the phase-picking algorithms are robust and effective in identifying the arrival times of the P and S phases.

Magnitude Estimation

Calculation of Parameters a and m to Estimate the Magnitude

At time i, when the P wave is detected, the process initiates the calculation of the two parameters used to estimate the magnitude range of the earthquake. For this purpose, the algorithm uses the sum of ASIV_{16} and ASIH_{16}, which is the cumulative average squared acceleration over the $2(t_S–t_P)$ time window. This function is related to the seismic energy released and is defined as a in equation (6).

The second parameter is the derivative m, estimated from the beginning of detection of the P wave to time $2(t_S–t_P)$ (equation 7) and measured at instant $i = 2(t_S–t_P)$.

$$a = \log_{10}\left[\sum_{i=t_P}^{2(t_S-t_P)} \mathrm{ASIV}_{16}(i) + \mathrm{ASIH}_{16}(i)\right] \quad (6)$$

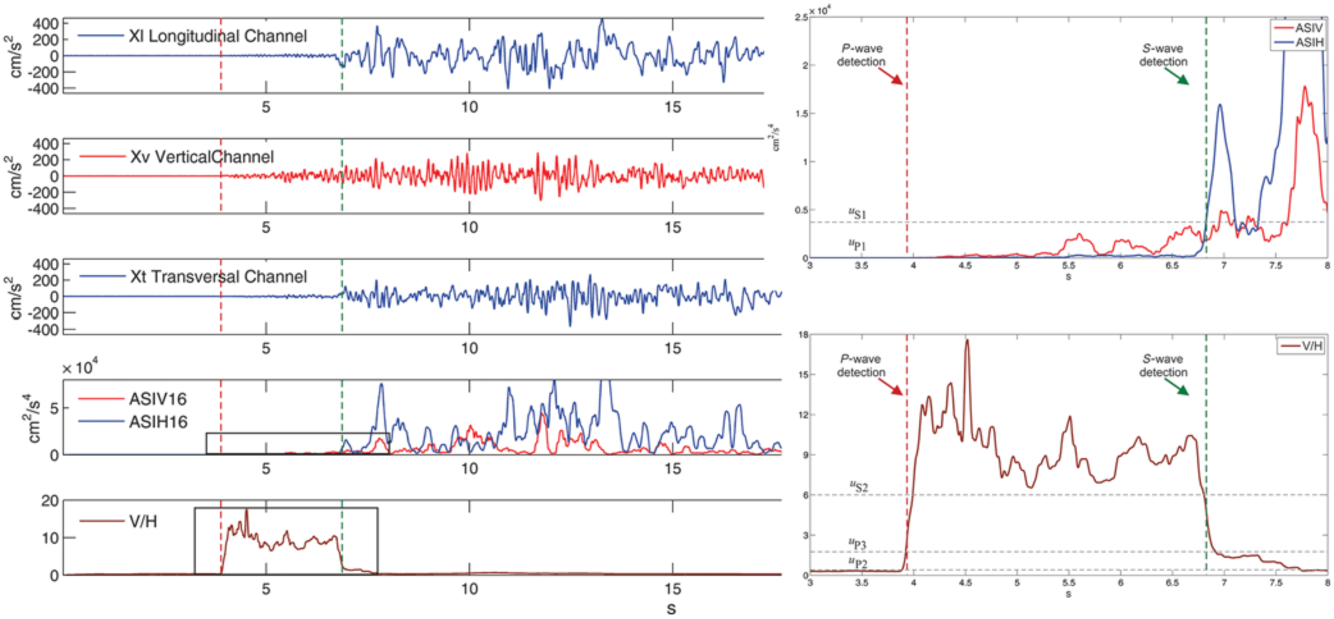

Figure 2. Example of P- and S-wave detection based on the $2(t_S–t_P)$ algorithm. The first three traces show accelerograms from station Cacalutla for the 13 April 2007 M_w 6.0 Atoyac, Guerrero, Mexico, earthquake. The two lower traces show the characteristic functions used for detecting P and S waves, which are amplified in the box.

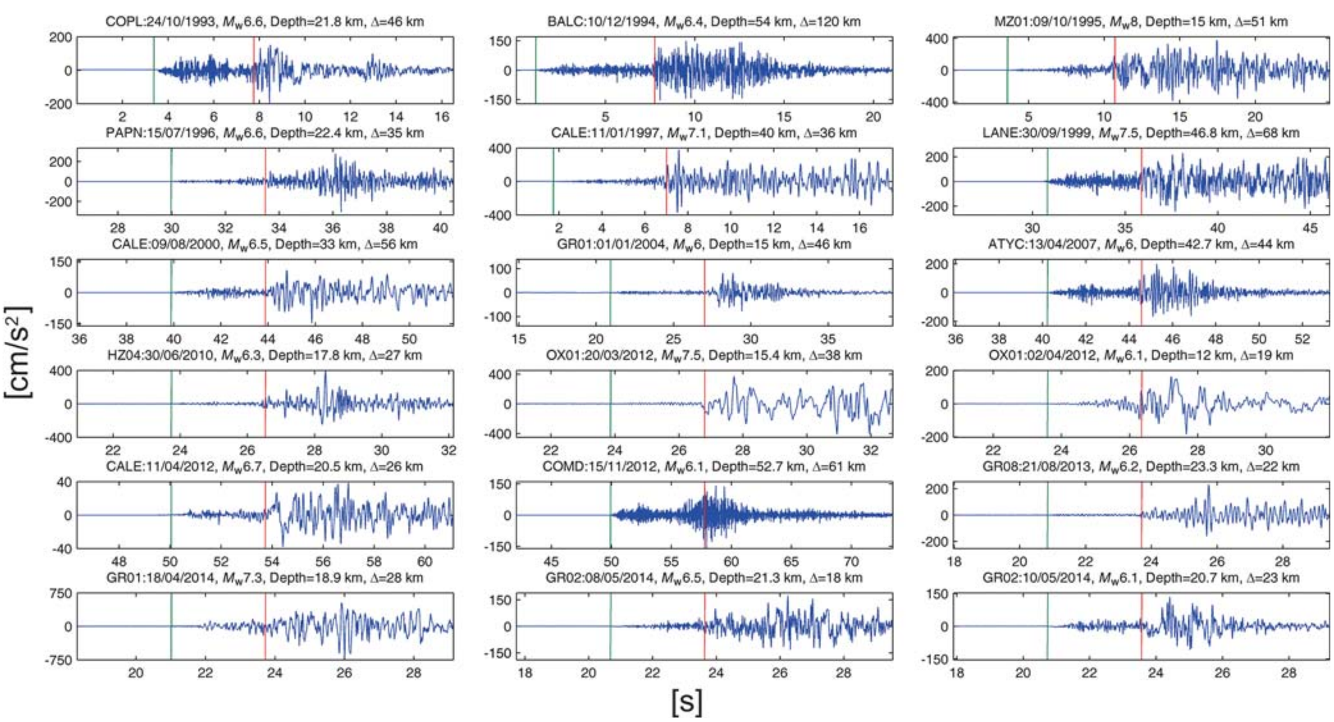

Figure 3. Strong-motion records of selected earthquakes analyzed in this study. The green and red tick marks show the arrival time of the P and S waves identified by the $2(t_S–t_P)$ algorithm.

$$m = \log_{10}[\mathrm{ASIV}_{16}(2(t_S–t_P)) + \mathrm{ASIH}_{16}(2(t_S–t_P))]. \quad (7)$$

As an example, the energy release parameter a is shown for the 13 April 2007 M_w 6.0 Atoyac earthquake (Fig. 4). The black arrow indicates the time when a and m were obtained.

Criterion for Alert Activation

The activation of the public or preventive alerts requires estimates of magnitude $m_{2(t_S-t_P)}$ in at least two seismic sensing stations close to the epicenter. This criterion prevents false alarms induced by failures in the electronic components

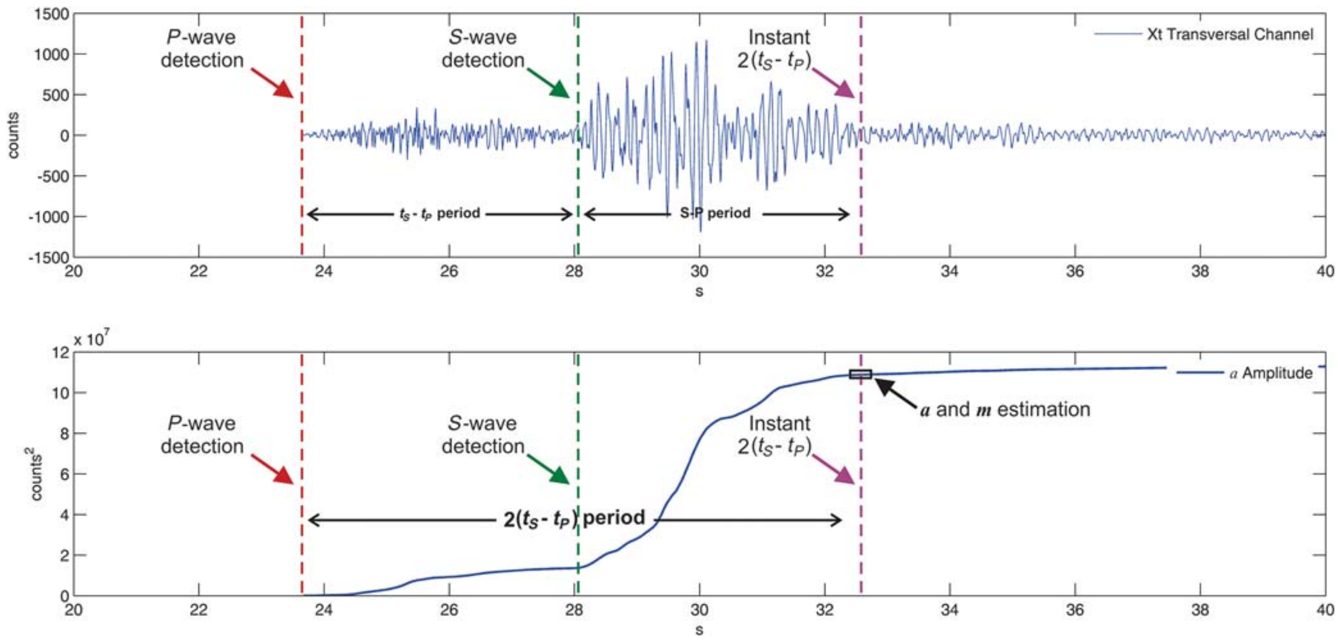

Figure 4. The upper trace shows an accelerogram of the 13 April 2007 M_w 6.0 earthquake. The box below shows the resulting function of the estimated quadratic amplitude a and instant rate of growth m calculated in the time period $2(t_S–t_P)$. The black arrow shows the time $2(t_S–t_P)$ when the parameters are calculated.

or by spurious seismic noise in one of the stations. In addition, it allows simultaneous monitoring of earthquakes in different regions, improving the coherence by geographically delimiting the observation of earthquakes. The algorithm has the additional advantage of requiring only two stations to detect and classify earthquakes. Most other systems make use of a higher number of stations to avoid false alerts.

A shortcoming of this confirmation criterion by more than one sensing station is the need to invest additional time for the activation of the alert. However, considering that today the average spatial separation of SASMEX strong-motion stations in the subduction zone is about 25 km, the time necessary to receive the confirmation of a second station is generally less than 2 or 3 s. During its operational history, SASMEX had only one false alert. It occurred on 16 November 1993, during its early stages of development, when only one FS station was required to activate the alert (Espinosa-Aranda *et al.*, 1995).

The $2(t_S–t_P)$ algorithm assumes that the energy released is empirically associated with the magnitude m_b. The original alerting rules established by the authorities of Mexico City for the design of the system were: not alerting earthquakes with $m_b < 5.0$, relaying a preventive alert if $5.0 \leq m_b < 6.0$, and activating a public alert when $m_b \geq 6.0$. The authorities set up this criteria after considering that the earthquakes of $m_b \geq 6.0$ in the Guerrero gap might cause damage and generally would be felt by everyone in Mexico City. On the other hand, earthquakes in the subduction zone of magnitude $5.0 \leq m_b < 5.5$ are usually felt only by people in the zones underlain by the soft soils. The motives behind issuing preventive alerts for this magnitude range were to promote the practice of seismic drills in schools. Today, the alerting policy for the $2(t_S–t_P)$ algorithm is as follows: no alert for earthquakes with $m_b < 5.5$; relay a preventive alert if $5.5 \leq m_b < 6.0$; and issue a public alert when $m_b \geq 6.0$.

The numerical model to estimate the magnitude is expressed as contours of the parameters a and m as a function of m_b. The contours used by SASMEX and tested in this article were calibrated (Espinosa-Aranda *et al.*, 1992) based on accelerograms of 12 earthquakes that occurred between 1985 and 1989 and recorded by strong-motion stations of the Accelerograph Network of the State of Guerrero (Anderson and Quaas, 1988). Magnitude m_b was used due to the scarce number of earthquakes registered by accelerographs that were operating during the early days of the warning system. Furthermore, m_b was the magnitude normally reported at the time for earthquakes with moderate magnitude by the various agencies responsible (Espinosa-Aranda *et al.*, 1992).

Although the algorithm has been improved, the equations derived from the classification functions to determine the range of magnitude remained unchanged. Equations (8)–(10) define the magnitude range $m_{2(t_S-t_P)}$ as a function of parameters a and m (Fig. 5). As mentioned before, $m_{2(t_S-t_P)}$ is proportional to magnitude m_b.

When the logic function is validated as TRUE by more than one equation, the largest magnitude value is assigned:

$$\text{if } a + m - 7 \geq 0; \text{ is TRUE then } m_{2(t_S-t_P)} \geq 5.0; \quad \text{else } m_{2(t_S-t_P)} < 5.0; \tag{8}$$

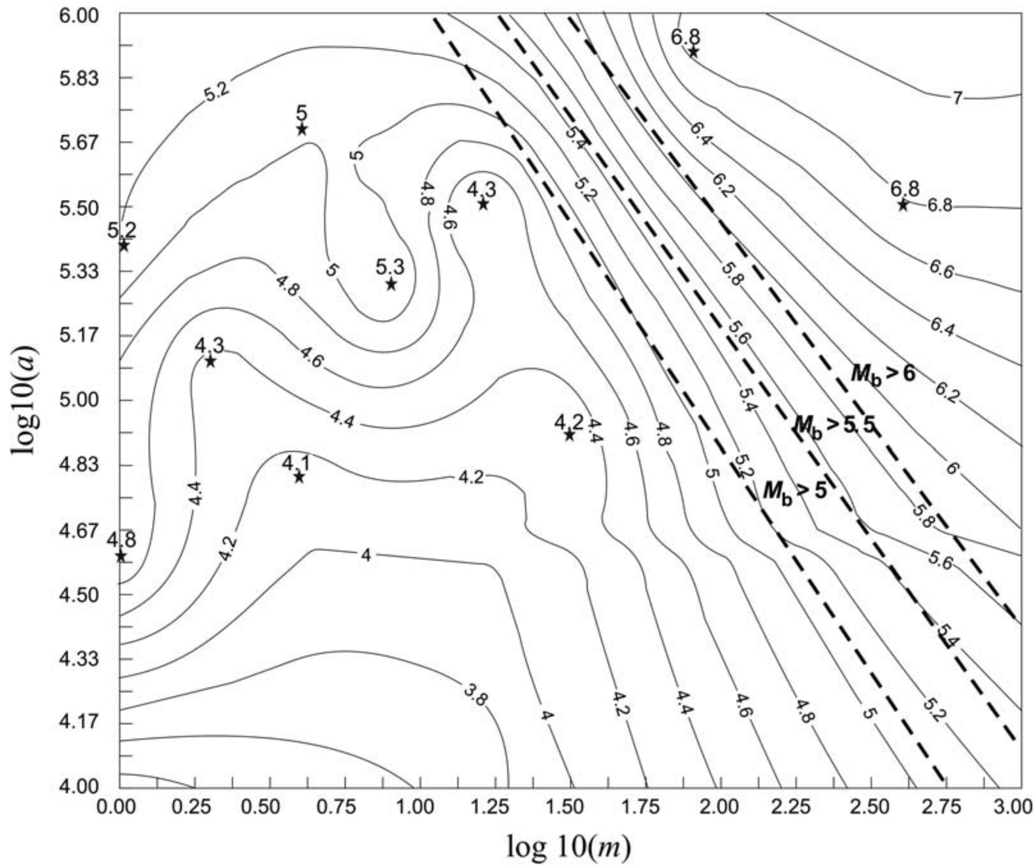

Figure 5. Magnitude m_b contours based on the parameters a and m. The calibration curves were estimated based on the data from 12 earthquakes occurring from 1985 to 1989, for which the epicenter lies at a distance of less than 80 km from the closest seismic sensors of the Guerrero strong-motion network (Anderson and Quaas, 1988).

if $a + 0.98m - 7.18 \geq 0$; is TRUE

$$\text{then } m_{2(t_S-t_P)} \geq 5.5; \tag{9}$$

if $a + m - 7.6 \geq 0$; is TRUE

$$\text{then } m_{2(t_S-t_P)} \geq 6.0. \tag{10}$$

Evaluation of the Performance of Algorithm $2(t_S–t_P)$

After almost 25 years of operation of SASMEX, it is important to conduct a systematic evaluation of its performance and, in particular, of the $2(t_S–t_P)$ algorithm used for detection and classification of earthquakes. To conduct a fair and objective test, the $2(t_S–t_P)$ algorithm was evaluated based on the same criteria, using the following datasets:

1. All earthquakes recorded by SASMEX strong-motion instruments during its history of operation (Ⓔ Tables S1 and S2).
2. All earthquakes of $M_w \geq 6.0$ which took place in the subduction zone but which were not recorded by the original SASMEX stations. In these cases, the tests were based on accelerograms of other strong-motion networks (Ⓔ Table S3). It should be emphasized that all earthquakes fulfilling these criteria were included without exceptions. This dataset includes the only subduction earthquakes of $M_w > 8.0$ recorded in Mexico by strong-motion instruments: the 9 October 1995 earthquake and the 19 September 1985 great Michoacán earthquake.
3. Also, we tested the robustness of the algorithm for great magnitude earthquakes using records of the 2010 M_w 8.8 Maule, Chile, earthquake and the 2011 M_w 9.0 Tohoku, Japan, earthquake.

Evaluation of the Magnitude Estimates Reported by SASMEX

Iglesias *et al.* (2007) and Suárez *et al.* (2009) argued that SASMEX magnitudes are not always accurate. Although magnitude determination is not the mission of SASMEX, it is important to reevaluate the capability of the algorithm $2(t_S–t_P)$ to classify and discriminate earthquakes in the magnitude bins established.

An analysis is presented of the alerts issued from 1991 to 2014. During that period, the algorithm discriminated over 5400 earthquakes and 8560 acceleration records. The following criteria were considered to develop a consistent database:

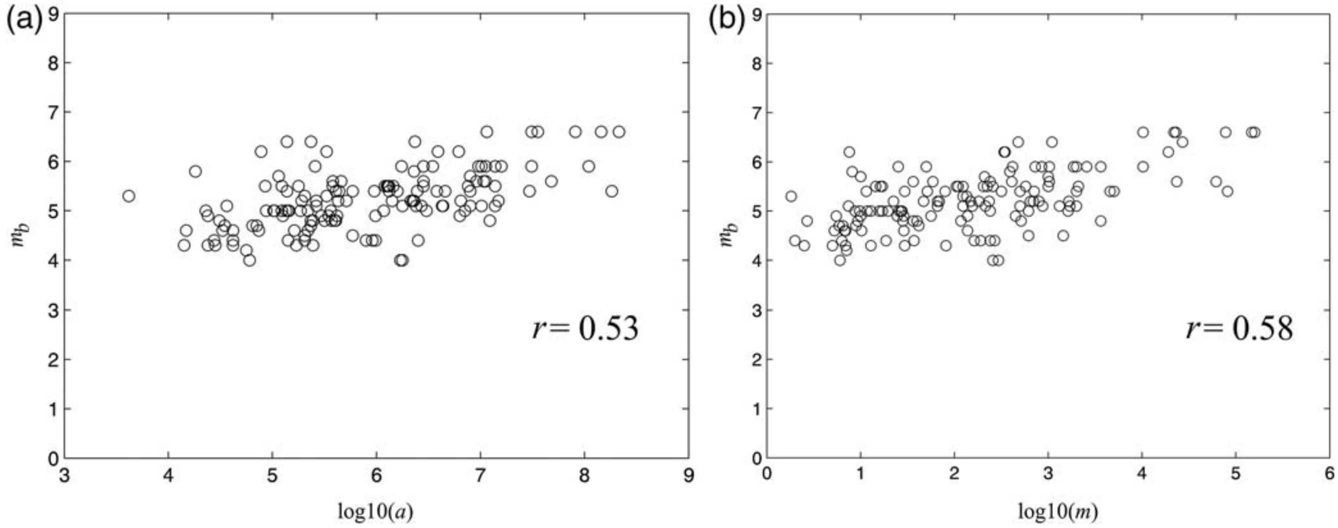

Figure 6. Correlation in a logarithmic scale between parameters based on 144 recordings: (a) m_b versus a and (b) m_b versus m.

1. All earthquakes in the subduction zone are selected that generated either public or preventive alerts in Mexico City and for which an m_b value is available from published seismic catalogs.
2. The accelerograms recorded by two of the early SASMEX stations (GR08 and GR12) are not used in the detection and classification algorithm because they suffer very large amplification effects due to local site conditions.

A total of 61 earthquakes met these criteria and were recorded in 144 strong-motion records (Ⓔ Table S2).

To estimate the correlation of the parameters a and m used as alerting criteria as a function of the observed magnitude m_b, the correlation criterion of Pearson was applied (Pearson, 1896). The correlation between parameters a and m observed in the 144 acceleration records used in the analysis (Ⓔ Table S2) shows a coefficient of $r = 0.53$, whereas the correlation of parameters m and m_b is equal to $r = 0.58$ (Fig. 6). These results show an acceptable degree of correlation between the parameters employed by the $2(t_S–t_P)$ algorithm and magnitude m_b. It should be noted that the correlation between parameters a and m is $r = 0.88$. The significant linear relationship between these two variables indicates that they are potentially redundant.

For the 61 earthquakes analyzed, a comparison is made between the magnitude m_b reported by the Servicio Sismológico Nacional (SSN) and other international agencies and the estimated magnitude range $m_{2(t_S–t_P)}$ (Ⓔ Table S2). Our results show that for the acceleration records of earthquakes with $m_b < 5.0$, 65% of the magnitudes predicted by the algorithm fall within ±0.5 units of the reported catalog magnitude. When the same evaluation is done for acceleration records of earthquakes with $m_b \geq 6.0$ and $m_b \geq 5.5$, the success rate increases to 92% and 83%.

The earthquake early warning system in Japan tolerates errors of ±1.0 in magnitude estimation (Hoshiba *et al.*, 2008). Assuming this same magnitude tolerance, the algorithm $2(t_S–t_P)$ has a success rate of 92% and 87% for $m_b \geq 6.0$ and $m_b > 5.5$, respectively. Thus, for the magnitude ranges used in the decision-making process of whether to issue public or preventive alerts, the $2(t_S–t_P)$ algorithm demonstrates that it is a robust and reliable tool to rapidly classify earthquakes into magnitude ranges and to issue alerts with a high degree of confidence.

Evaluation of Mexican Subduction Earthquakes with $M_w \geq 6.0$ since 1985

In the first 24 years of operation, the coverage of SASMEX was limited to 12 strong-motion sensors located to the southeast of Acapulco (Espinosa-Aranda *et al.*, 1995). Many subduction earthquakes of $M_w \geq 6.0$ took place outside the zone originally covered by SASMEX. To test the performance of the algorithm on these earthquakes, we obtained and processed the acceleration records of these earthquakes recorded by other strong-motion networks.

According to the centroid moment tensor catalog (Dziewonski *et al.*, 1981, 1999; Ekström *et al.*, 2012), 41 earthquakes ($M_w \geq 6.0$) took place from 1985 to 2014 along the Mexican subduction zone. Out of these 41 earthquakes, 31 of them were recorded on 59 acceleration records (Fig. 7 and Ⓔ Table S3). The earthquakes to be evaluated were chosen based on the following criteria:

1. earthquakes of $M_w \geq 6.0$ occurring since September 1985 along the Mexican subduction zone;
2. earthquakes for which the distance between the epicenter and Mexico City is less than 600 km; and
3. earthquakes for which two seismic stations are located close to the epicenter, within a maximum distance of 120 km and for which the acceleration recordings show both the P and S waves.

The two stations closest to the epicenter were selected whenever $t_S–t_P$ times were available. Most of the records are from

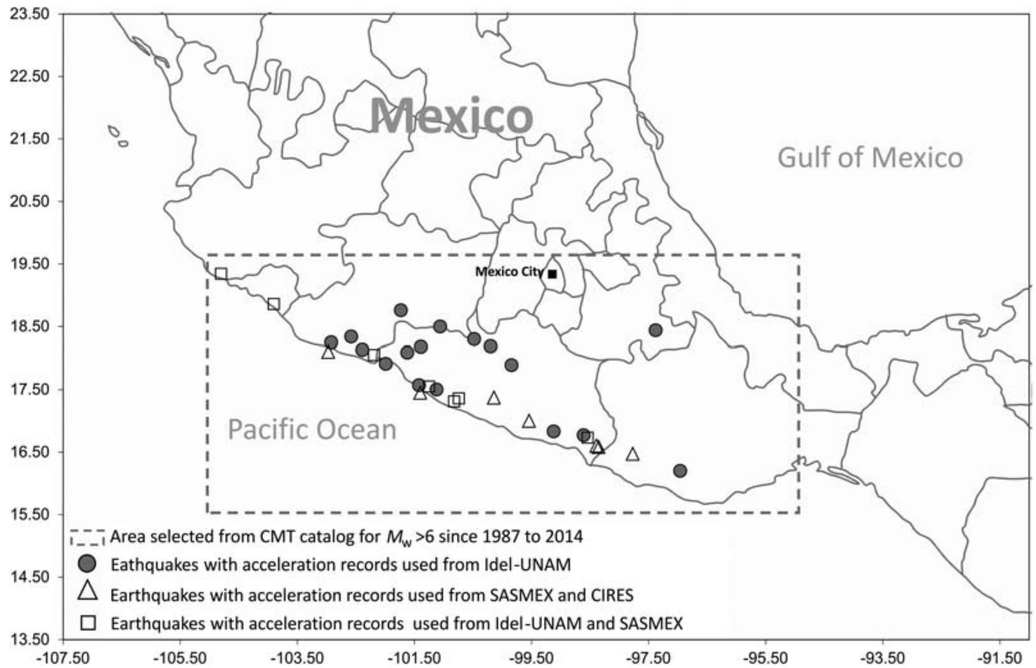

Figure 7. Location of the earthquakes with $M_w \geq 6.0$ used in the analysis, which have occurred in southern Mexico since 1985.

the strong-motion networks operated by the Instituto de Ingeniería, Universidad Nacional Autónoma de México (Pérez-Yáñez *et al.*, 2014) and by the SASMEX network managed by CIRES. The majority of these earthquakes are located at distances of less than 50 km from the closest strong-motion station (Ⓔ Table S3). Among these earthquakes, there are seven earthquakes of $M_w \geq 7.0$, all strongly felt in Mexico City. The summarized results obtained with algorithm $2(t_S–t_P)$ are shown in Figure 8.

For both the great 19 September 1985 M_w 8.1 Michoacán earthquake and the 9 October 1995 M_w 8.0 Colima earthquake, the algorithm $2(t_S–t_P)$ determined a magnitude range of $m_{2(t_S-t_P)} > 6.0$, even though the strong-motion stations were few and located far from the epicenter. Although the magnitude of these two large events based only on the existing accelerograms is severely underestimated, the $2(t_S–t_P)$ algorithm would have triggered a public alert, had it been operating at the time. Even under these unfavorable conditions, the warning time in Mexico City for these two earthquakes would have been 90–110 s.

In the case of the 19 September 1985 event, acceleration records exist for stations CALE and ZACA. These stations are located at a distance of 40 and 57 km, respectively. CALE was the only station for which both P and S waves were recorded. In ZACA, the station triggered after the arrival of the P wave. The low accelerations observed in CALE were attributed to the fact that the nucleation of the 1985 earthquake was located beneath station CALE (Mendez and Anderson, 1991); the value of parameter a for the 1985 event is smaller than that observed for 21 September (M_w 7.6) (Fig. 8). Similarly, a slow growth in seismic energy was observed in stations located close to the hypocenter of other large earthquakes such as the 20 March 2012 (M_w 7.4) event recorded by station OX01 at a distance of 42 km from the epicenter (Fig. 8).

The results of the evaluation of the $2(t_S–t_P)$ algorithm performed on earthquakes of $M_w \geq 6.0$ (Ⓔ Table S3) show that the magnitudes were classified consistently by the algorithm as $m_{2(t_S-t_P)} \geq 6.0$. The only exception is the earthquake of 9 August 2000 (M_w 6.5) in the state of Michoacán, where the algorithm $2(t_S–t_P)$ estimated a magnitude $m_{2(t_S-t_P)} \geq 5.5$ in one of the two acceleration records used (Fig. 8). This result is probably due to the fact that the second closest station to the epicenter (UNIO station) is located 90 km from the epicenter.

The results obtained demonstrate that the algorithm is robust and correctly identifies and classifies large-magnitude earthquakes. Our results show also that more accurate magnitudes are obtained for earthquakes with $M_w \geq 6.0$, when there are stations located close to the epicenter. The current average separation of SASMEX sensing stations along the subduction zone is ~25 km. This spacing gives confidence that future large-magnitude earthquakes will be properly identified and discriminated to issue a public alert.

Performance of the Magnitude Classification Algorithm for Earthquakes with $M_w \geq 6$

The tests described above confirm the robustness of the algorithm to identify large earthquakes ($M_w \geq 6$). However, it is important to test whether it is effective also in classifying small-magnitude earthquakes in the subduction zone. To this end, it is worth mentioning that from 1991 to 2014, the SASMEX network detected ~5400 earthquakes; the majority of

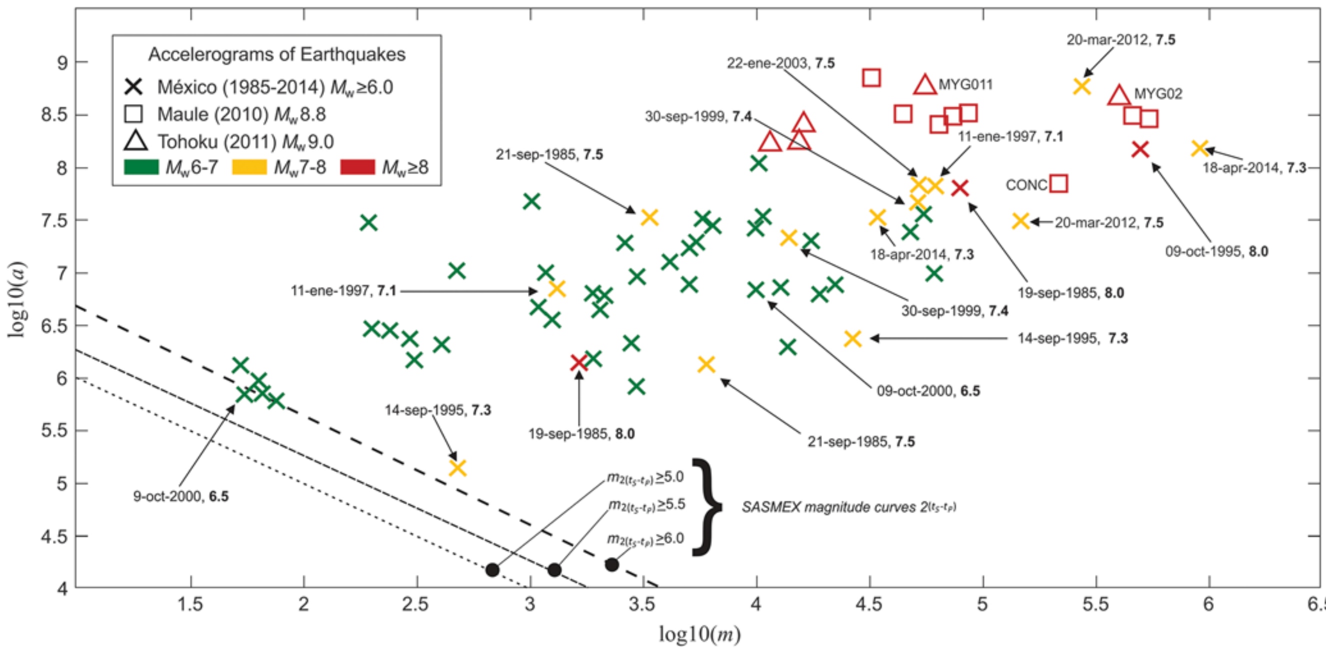

Figure 8. Magnitude estimated based on the $2(t_S–t_P)$ algorithm based on the accelerograms of earthquakes $M_w \geq 6.0$, which occurred in Mexico from 1985 to 2014, as well as for the 2010 M_w 8.8 Chile earthquake and the 2011 M_w 9.0 Tohoku event.

which are $M_w < 5$. Out of these 5400 earthquakes, SASMEX issued only 92 alerts based on the $2(t_S–t_P)$ algorithm (see Data and Resources). These results indicate that it correctly discriminates small earthquakes of $M_w < 5$ and does not emit an alert to the population.

As mentioned before, the coverage of the SASMEX system was considerably expanded and improved in 2013, and the alerting criteria were modified at the same time. The system now covers the whole Mexican subduction zone (Fig. 1). To further illustrate the ability of the $2(t_S–t_P)$ algorithm to discriminate the prescribed magnitude bins, the earthquakes recorded by SASMEX from 2013 to August 2016 are classified by year and magnitude range (Table 1). The magnitude values used are those reported by the SSN. The dataset covers 710 earthquakes recorded in the last four years. These data are detected based on the current distribution of SASMEX stations and the alerting criteria used today. This allows a fair and homogeneous comparison of the performance of the algorithm (Table 1).

To facilitate the analysis, a confusion matrix was constructed to compare the various alerts issued during this same period (Table 2). The elements along the diagonal of the matrix reflect earthquakes which were correctly classified. Out of the 710 events detected within this period, 701 were correctly screened out as earthquakes for which no alert was issued. Also, the five earthquakes with $M_w \geq 6$, which occurred during this period, were correctly identified as deserving public alerts. The elements off the diagonal of the matrix are those earthquakes incorrectly classified. In all cases, the events misclassified are in the magnitude bin $5.5 \leq M_w < 6.0$, in which preventive alerts should be issued. In the case of two events in this magnitude range, the algorithm incorrectly issued a public alert. In two other cases, no alert was issued when a preventive alert should have been emitted.

Table 1
Alerts Issued by the $2(t_S–t_P)$ Algorithm in the Mexican Subduction Zone by Alert Category and Magnitude

M_w	2013		2014		2015		2016	
≥ 6.0	Public	1	Public	3	Public		Public	1
	Preventive		Preventive		Preventive		Preventive	
	No alert		No alert		No alert		No alert	
$5.5 \leq M_w < 6.0$	Public		Public		Public	1	Public	1
	Preventive		Preventive		Preventive		Preventive	
	No alert		No alert	2	No alert		No alert	
< 5.5	Public		Public		Public		Public	
	Preventive		Preventive		Preventive		Preventive	
	No alert	275	No alert	169	No alert	140	No alert	117

Table 2
Alerts Issued by the $2(t_S–t_P)$ Algorithm from January 2013 to August 2016

SASMEX Warning	$M_w < 5.5$	$5.5 \le M_w < 6.0$	$M_w \ge 6.0$
No alert	701	2	0
Preventive	0	0	0
Public	0	2	5

SASMEX, Seismic Alert System of Mexico.

These errors reflect the difficulties of the algorithm to correctly classify earthquakes within this very narrow magnitude range. In fact, a discussion is taking place as to whether preventive alerts should continue to be emitted based on this narrow magnitude range, or whether SASMEX should only issue public alerts for events $m_b < 5.5$, eliminating preventive alerts. Regardless, the results of the past four years show that the $2(t_S–t_P)$ algorithm is a reliable tool that correctly classifies earthquakes to issue alerts of large incoming earthquakes.

Evaluation of the 2010 M_w 8.8 Maule Earthquake

The 27 February 2010 M_w 8.8 Chile earthquake occurred in the Maule region in central Chile (e.g., Delouis *et al.*, 2010). With the idea of testing the $2(t_S–t_P)$ algorithm for great earthquakes, we obtained and processed eight acceleration records observed along the coast of Chile (Ⓔ Table S4; Boroschek *et al.*, 2012). The acceleration recording stations closest to the epicenter are in the cities of Concepción (CONC) and Constitución (CONT), at epicentral distances of 108 and 78 km, respectively (Ⓔ Fig. S3 and Ⓔ Table S4). P waves are not identifiable on most of these accelerograms. Furthermore, the distances between the epicenter and the closest stations fall outside the design parameters of the $2(t_S–t_P)$ algorithm.

Despite these unfavorable conditions, the algorithm classified the Maule earthquake as magnitude $m_{2(t_S-t_P)} \ge 6.0$, even at strong-motion stations located at distances of 270 km from the epicenter (Ⓔ Fig. S3 and Ⓔ Table S4). If SASMEX had been in operation at that time, even with this unfavorable station distribution, a public alert would have been issued for the Maule earthquake.

Evaluation of the 2011 M_w 9.0 Tohoku Earthquake

On 11 March 2011, the region of Tohoku, Japan, along the coast of Honshu suffered an earthquake of M_w 9.0 (e.g., Mori *et al.*, 2011). The fault was located up-dip of the subduction zone, close to the trench. Because of this, the distance between the strong-motion stations on land and the rupture zone is very large. Thus, this earthquake represents an extreme test for the robustness of the algorithm. Five acceleration records were obtained from the stations closest to the epicenter. These strong-motion stations are part of Japan's earthquake early warning system (Hoshiba *et al.*, 2011).

The closest accelerographs are located at distances of more than 100 km from the epicenter (Ⓔ Fig. S4 and Ⓔ Table S5). Consequently, the $(t_S–t_P)$ time is ~20 s. Despite this disadvantageous situation, the magnitude was classified as $m_{2(t_S-t_P)} \ge 6.0$ at all stations (Ⓔ Table S5). Although the magnitude is again severely underestimated, the algorithm would have been able to discriminate the Tohoku event as a very large earthquake and would have issued a public alert. Evidently, because of the large distances between the epicentral area and the closest seismic sensing stations on land, the warning time for Tokyo and neighboring cities would have been only a few seconds.

Summary and Conclusions

Since the beginning of operations in 1991, SASMEX has used an algorithm which, based on the quadratic sum of the amplitude of the acceleration of the three orthogonal components in the period $2(t_S–t_P)$, discriminates and classifies the magnitude based on two parameters: the amplitude a and the instantaneous rate of growth of the energy m. Originally, these parameters are used to classify the earthquakes into magnitude ranges: $m_b < 5.0$, $5.0 \le m_b < 6.0$, and $m_b \ge 6.0$. No alert is issued in the first case and either a preventive or a public alert is issued for the two last instances, respectively. Today, the ranges for $2(t_S–t_P)$ algorithm are modified as $m_b < 5.5$, $5.5 \le m_b < 6.0$, and $m_b \ge 6.0$ considering the distance of 450 km or more of Mexico City.

The results presented here show that parameters a and m provide the basis for an adequate estimate of magnitude ranges for the alerting criteria used by SASMEX. Nevertheless, it should be mentioned that there is a high linear dependence between these parameters. This may be the reason for the less successful discrimination of earthquakes in a magnitude range $m_b < 6.0$. The performance analysis of magnitude estimation based on the $2(t_S–t_P)$ algorithm, accepting an error of ± 0.5, shows a success rate of 92% for magnitude range $m_b > 6.0$ and 83% for magnitude range $m_b > 5.5$ for the acceleration records analyzed. In the case of an error tolerance of ± 1.0 in magnitude, the estimation success rate reaches almost 92% and 87% for magnitude range $m_b > 6.0$ and $m_b > 5.5$, respectively.

A performance test was conducted based on 52 acceleration recordings corresponding to all earthquakes with $M_w \ge 6.0$ located along the Mexican subduction zone (Fig. 8 and Ⓔ Table S3). When executing the alerting algorithm $2(t_S–t_P)$ retroactively on these strong-motion records, all earthquakes, with a single exception in one acceleration record, were classified as being in the magnitude range of $m_{2(t_S-t_P)} \ge 6.0$. The only accelerogram not properly classified ($m_{2(t_S-t_P)} \ge 5.5$) has a very large epicentral distance to the closest strong-motion station. In the case of some large earthquakes, magnitudes are underestimated due to the greater magnitude range of the algorithm, precisely $m_{2(t_S-t_P)} \ge 6.0$.

Also, *post facto* performance tests were conducted using the $2(t_S–t_P)$ algorithm for the great Chile (M_w 8.8) and Tohoku (M_w 9.0) earthquakes. These performance tests represent extreme examples due to the very large distances between the strong-motion stations and the epicenters. Nonetheless, both earthquakes were classified in the magnitude range $m_{2(t_S-t_P)} > 6.0$ (Fig. 8; Ⓔ Tables S4 and S5). These results suggest that, even under quite unfavorable conditions, the method is robust enough to identify great earthquakes and issue a public alert. It should be stressed, however, that in these two scenarios, in which the earthquake occurs far from the seismic sensing stations, the algorithm $2(t_S–t_P)$ would not be suitable to issue a timely alert. We are currently working on faster algorithms for events in which $t_S–t_P$ is large.

The most important conclusion of this performance evaluation is that for the station versus epicentral distances found in the Mexican subduction zone, the $2(t_S–t_P)$ algorithm is robust and reliable. There are two main reasons behind this: first, the short distance between the hypocenters of large subduction earthquakes and the seismic sensing stations installed along the coast results in $t_S–t_P$ times that are usually less than 3–4 s. Second, the distance between the subduction zone and Mexico City allows ample warning time to issue an alert prior to the initiation of strong shaking. Finally, it is worth mentioning that the current station distribution of SASMEX records an average of 500 earthquakes per year in the subduction zone. Out of this large number of earthquakes, only a handful of seismic alerts are issued.

Data and Resources

Accelerograms from the Seismic Alert System of Mexico (SASMEX) stations were provided by the Centro de Instrumentación y Registro Sísmico (CIRES) with the authorization of the Instituto para la Seguridad en las Construcciones del Distrito Federal in Mexico City and the Coordinación Estatal de Protección Civil de Oaxaca in Oaxaca state. Strong-motion data for the Mexican subduction earthquakes are from the web page of the Instituto de Ingeniería of the Universidad Nacional Autónoma de México (UNAM) https://aplicaciones.iingen.unam.mx/AcelerogramasRSM/Default.aspx (last accessed December 2016). The National Accelerograph Network and the Seismological Service of the Universidad de Chile provided the strong-motion data for the Chilean earthquake. The Japanese accelerograms are from the National Research Institute for Earth Sciences and Disaster Prevention, Japan. Data from the Global Centroid Moment Tensor Project are from http://www.globalcmt.org/CMTsearch.html (last accessed December 2016). SASMEX historical catalog of alerts is available at http://www.cires.org.mx/sasmex_historico_es.php (last accessed December 2016).

Acknowledgments

The authors express their gratitude to the institutions that provided the strong-motion data: the Mexico City and Oaxaca governments (who allowed us to use the waveform database of the Seismic Alert System of Mexico [SASMEX]), the Instituto de Ingeniería of the National University of Mexico (UNAM), the Japan Meteorological Agency (JMA), and the National Research Institute for Earth Science and Disaster Prevention of Japan (NIED). The authors thank S. Barrientos for data from the National Accelerograph Network of the Department of Civil Engineering (RENADIC) and the Seismological Service at the Department of Geophysics (GUC), both of the Universidad de Santiago, Chile. G. S. acknowledges the Consejo Nacional de Ciencia y Tecnología (CONACYT) Grant 082821. A. C. acknowledges support of Centro de Instrumentación y Registro Sísmico (CIRES). The authors appreciate the comments and suggestions made by the anonymous reviewers, which helped improve the quality of this article.

References

Allen, R. M., H. Brown, M. Hellweg, O. Khainovski, P. Lombard, and D. Neuhauser (2009). Real-time earthquake detection and hazard assessment by ElarmS across California, *Geophys. Res. Lett.* **36,** no. 5, doi: 10.1029/2008GL036766.

Anderson, J. G., and R. Quaas (1988). The Mexico earthquake of September 19, 1985—Effect of magnitude on the character of strong ground motion: An example from the Guerrero, Mexico strong motion network, *Earthq. Spectra* **4,** no. 3, 635–646.

Boroschek, R. L., V. Contreras, D. Y. Kwak, and J. P. Stewart (2012). Strong ground motion attributes of the 2010 M_w 8.8 Maule, Chile, earthquake, *Earthq. Spectra* **28,** no. S1, S19–S38.

CONACYT-NRC (1986). Investigación para aprender de los sismos de septiembre 1985 en México, *Informe técnico preparado por comités conjuntos del Consejo Nacional de Ciencia y Tecnología (México) y el National Research Council (EUA)*, México (in Spanish).

Cuéllar, A., J. M. Espinosa-Aranda, G. Suárez, G. Ibarrola, A. Uribe, F. H. Rodríguez, and B. Frontana (2014). The Mexican Seismic Alert System (SASMEX): Its alert signals, broadcast results and performance during the *M* 7.4 Punta Maldonado earthquake of March 20th, 2012, in *Early Warning for Geological Disasters*, F. Wenzel and J. Zschau (Editors), Springer, Berlin, Germany, 71–87 pp.

Delouis, B., J. M. Nocquet, and M. Vallée (2010). Slip distribution of the February 27, 2010 $M_w = 8.8$ Maule earthquake, central Chile, from static and high-rate GPS, InSAR, and broadband teleseismic data, *Geophys. Res. Lett.* **37,** no. 17, doi: 10.1029/2010GL043899.

Dziewonski, A. M., T.-A. Chou, and J. H. Woodhouse (1981). Determination of earthquake source parameters from waveform data for studies of global and regional seismicity, *J. Geophys. Res.* **86,** 2825–2852, doi: 10.1029/JB086iB04p02825.

Dziewonski, A. M., G. Ekström, and N. N. Maternovskaya (1999). Centroid-moment tensor solutions for April–June, 1998, *Phys. Earth Planet. In.* **112,** no. 1, 11–19.

Ekström, G., M. Nettles, and A. M. Dziewonski (2012). The global CMT project 2004–2010: Centroid-moment tensors for 13,017 earthquakes, *Phys. Earth Planet. In.* **200/201,** 1–9, doi: 10.1016/j.pepi.2012.04.002.

Espinosa-Aranda, J. M., A. Cuellar, A. Garcia, G. Ibarrola, R. Islas, S. Maldonado, and F. H. Rodriguez (2009). Evolution of the Mexican seismic alert system (SASMEX), *Seismol. Res. Lett.* **80,** no. 5, 694–706.

Espinosa-Aranda, J. M., A. Jimenez, O. Contreras, G. Ibarrola, and R. Ortega (1992). Mexico City Seismic Alert System, International Symposium on Earthquake Disaster Prevention 18–21 May 1992, Mexico, *Proc. Centro Nacional de Prevención de Desastres and Japan International Cooperation Agency (CENAPRED-JICA)*, Mexico, Vol. I, 315–324.

Espinosa-Aranda, J. M., A. Jimenez, G. Ibarrola, F. Alcantar, A. Aguilar, M. Inostroza, and S. Maldonado (1995). Mexico City seismic alert system, *Seismol. Res. Lett.* **66,** no. 6, 42–53.

Esteva, L. (1988). The Mexico earthquake of September 19, 1985—Consequences, lessons and impact on research and practice, *Earthq. Spectra* **4,** no. 3, 413–426.

Hoshiba, M., K. Iwakiri, N. Hayashimoto, T. Shimoyama, K. Hirano, Y. Yamada, and H. Kikuta (2011). Outline of the 2011 off the Pacific coast of Tohoku Earthquake (M_w 9.0)—Earthquake early warning and observed seismic intensity, *Earth Planets Space* **63,** no. 7, 547–551.

Hoshiba, M., O. Kamigaichi, M. Saito, S. Y. Tsukada, and N. Hamada (2008). Earthquake early warning starts nationwide in Japan, *Eos Trans. AGU* **89,** no. 8, 73–74.

Iglesias, A., S. K. Singh, M. Ordaz, M. A. Santoyo, and J. Pacheco (2007). The seismic alert system for Mexico City: An evaluation of its performance and a strategy for its improvement, *Bull. Seismol. Soc. Am.* **97,** no. 5, 1718–1729.

McCann, W. R., S. P. Nishenko, L. R. Sykes, and J. Krause (1979). Seismic gaps and plate tectonics: Seismic potential for major boundaries, *Pure Appl. Geophys.* **117,** no. 6, 1082–1147.

Mendez, A. J., and J. G. Anderson (1991). The temporal and spatial evolution of the 19 September 1985 Michoacan earthquake as inferred from near-source ground-motion records, *Bull. Seismol. Soc. Am.* **81,** no. 3, 844–861.

Mori, N., T. Takahashi, T. Yasuda, and H. Yanagisawa (2011). Survey of 2011 Tohoku earthquake tsunami inundation and run-up, *Geophys. Res. Lett.* **38,** no. 7, doi: 10.1029/2011GL049210.

Nakamura, Y. (1996). Real-time information systems for seismic hazards mitigation UrEDAS, HERAS and PIC, *Quarterly Report-RTRI*, Vol. 37, 112–127.

Pearson, K. (1896). Mathematical contributions to the theory of evolution. III. Regression, heredity and panmixia, *Phil. Trans. Roy. Soc. London* **187,** 253–318.

Pérez-Yañez, C., L. Ramirez-Guzman, A. L. Ruiz, R. Delgado, M. A. Macías, H. Sandoval, L. Alcantara, and A. Quiroz (2014). Strong ground motion database system for the Mexican seismic network, presented at the *AGU Fall Meeting*, 14–19 December, San Francisco, California.

Rosenblueth, E. (1986). The 1985 earthquake: Causes and effects in Mexico City, *J. Am. Concr. Inst.* **8,** no. 5, 23–24.

Singh, S. K., L. Astiz, and J. Havskov (1981). Seismic gaps and recurrence periods of large earthquakes along the Mexican subduction zone: A reexamination, *Bull. Seismol. Soc. Am.* **71,** no. 3, 827–843.

Suárez, G., D. Novelo, and E. Mansilla (2009). Performance evaluation of the seismic alert system (SAS) in Mexico City: A seismological and a social perspective, *Seismol. Res. Lett.* **80,** no. 5, 707–716.

Instituto de Geofísica
Universidad Nacional Autónoma de México
Ciudad Universitaria
Mexico CDMX 04510
cuellara@cires.org.mx
gerardo@geofisica.unam.mx
(A.C., G.S.)

Centro de Instrumentación y Registro Sísmico
Anaxágoras 814
Colonia Narvarte
México CDMX 03020
espinosajm@cires.org.mx
(J.M.E.-A.)

Manuscript received 23 November 2015;
Published Online 7 March 2017